IETE Technical Review

ISSN: (Print) (Online) Journal homepage: https://www.tandfonline.com/loi/titr20

A Communication-assisted Scheme in Radial Distribution Systems Using Phasor Measurement Units

Alok Jain & M.K. Verma

To cite this article: Alok Jain & M.K. Verma (2020) A Communication-assisted Scheme in Radial Distribution Systems Using Phasor Measurement Units, IETE Technical Review, 37:5, 489-503, DOI: 10.1080/02564602.2019.1660237

To link to this article: https://doi.org/10.1080/02564602.2019.1660237

IETE TECHNICAL REVIEW
2020, VOL. 37, NO. 5, 489–503
https://doi.org/10.1080/02564602.2019.1660237

A Communication-assisted Scheme in Radial Distribution Systems Using Phasor Measurement Units

Alok Jain and M.K. Verma

Department of Electrical Engineering, Indian Institute of Technology (BHU), Varanasi 221 005, India

ABSTRACT

Automation of the distribution system may be an essential requirement in the smart grid architecture. In this paper, the architecture of the distribution system has been proposed, where Phasor Measurement Unit (PMU) has been placed at the main substation receiving supply from the grid through the incoming feeder, as well as at all distribution transformers (DTs). PMU installed at the main substation is linked to master controller through IEC 61850. PMUs placed at DTs are connected to the corresponding local controller through the IEC 61850. Estimated voltage and current phasors together with frequency are transmitted from PMU to the local controller through IEC 61850 communication protocol. Controllers perform different tasks based on the data received from PMUs. Each local controller is linked to master controller as well as to all smart meters placed at loads supplied by the DT. Bidirectional exchange of information takes place between master and local controllers as well as between local controller and smart meter. PMUs are also linked with the smart meters using PLC communication link. In this paper, information about the available power at the substation and at the distribution transformer is developed in real-time with the help of PMU by considering the load disconnection/connection based on available power (from time $t = 0.56$sec to time $t = 0.75$sec), protection of feeder against overcurrent (from time $t = 0.15$sec to time $t = 0.20$sec), and power theft detection and elimination (from time $t = 0.21$sec to time $t = 0.23$sec) through eMEGASim® OP5600 OPAL-RT real-time simulator.

KEYWORDS

Available power loss; Distribution system; Phasor measurement unit (PMU); Protocol; Smart metering; IEC 61850

NOMENCLATURE

PMUs	Phasor measurement units
DTs	Distribution transformers
DSM	Demand-side management
DRM	Demand response management
RESs	Renewable energy resources
HLM	Home load management
LV	Low voltage
DMS	Distribution management systems
SCADA	Supervisory control and data acquisition system
PQ	Power quality
UTC	Universal time coordinated
ROCOF	Rate of change of frequency
PDC	Phasor data concentrator
IEDs	Intelligent electronic devices
LAN	Local area network
GOOSE	Generic object-oriented substation event
SMV	Sampled measured value
MMS	Manufacturing message specification
MUs	Merging units
CTs	Current transformers
VTs/PTs	Voltage/Potential transformers
CB	Circuit breaker
PLL	Phase-locked loop
IGEC	Indian electricity grid code
SAS	Substation automation system

1. INTRODUCTION

A framework for autonomous DSM, that adopts a structure with admission management, load equalization, and DRM has been conferred in [1,2], wherever the native utility will coordinate power production and consumption through demand response systems and therefore the customers will balance the power request by integration native RESs and storage devices into the formulation of load equalization and admission management. But, the problems associated with challenges like detection and elimination of theft, protection of feeder against overcurrent got to be addressed. A distributed system-wide DRM algorithm to coordinate the operation of residential

This article was originally published with errors, which have now been corrected in the online version. Please see Correction (http://dx.doi.org/10.1080/02564602.2020.1827709)

HLM modules in an intelligent grid has been conferred [3,4]. This developed algorithm enhances the overall load profile, network voltage magnitudes, and network losses. However, varied network challenges like load equalization, overcurrent protection, and theft detection haven't been thought of. Totally different techniques are used for identification of phases to balance the actual phase in distribution grids [5–8]. However, these approaches don't investigate the performance exploitation real metering information obtained from each transformers and houses. A cost efficient idea as a metric of the economic cost of electricity consumption to optimize the consumption profit per cost has been planned [9]. However, in conjunction with load shifting and balancing, the author solely considers the residential consumption, but this approach doesn't investigate the performance using real-time metering information. The fundamental issues for the good metering applications in business and residential buildings are planned [10]. However, numerous network challenges like load balancing, overcurrent protection, and theft detection haven't been thought-about, and also the author doesn't investigate the performance in real time system. A survey on smart metering and its information analytics has been bestowed [11], in which some completely different smart meter technologies are highlighted, however, the author doesn't think about the privacy of the shoppers, and conjointly he doesn't consider the real-time communication protocols for the transfer of information. The author planned a replacement of meter with smart meters which may have good compression rates, conjointly giving observability options in LV DMS/SCADA [12], in which smart metering becomes associate degree enabler of voltage management needed by active distribution grids. But, the author doesn't think about the communication protocols for the transfer of information. A finite mixture model based mostly clump of residential customers exploitation smart meter measurements considering the behavior of customers in several time-periods has been planned [13]. However, clusters therefore fashioned haven't been tested in observance, control, and protection of real-time systems. The doable adverse consequences for PQ of introducing smart-grid technologies and applications are thought-about [14]. General protection themes for loop-based small grids are planned [15], which analyses the variations in voltages, currents, and frequencies between grid-connected mode and island mode. However, the author didn't embody numerous operational conditions, like unbalancing of loads, completely different earth-connection systems, special management methods, and conjointly to verify the results with the real-time system. A replacement in consumption pattern-based energy-theft detector has been bestowed [16] that depends on the certainty of customer's traditional and malicious usage patterns. However, this approach does not investigate the performance using real-time smart metering data. It also does not give theft notification with certain time period 't' to the control center and also to the customers. According to C37.118.1-2011 Std. of IEEE [17], PMUs are measurement devices capable of providing UTC time-tagged estimation of frequency, ROCOF, voltage/current phasors and streaming them to a concentration point. The high rates of reporting as well as accuracy of the PMUs data make PMU suitable for operators of distribution & transmission networks for real-time monitoring, control and protection functionalities. The PDC needs to operate synchronously as well and the synchronization can either be given by the synchronous PMU data flow itself or by properly synchronizing the PDC to a traceable UTC-time source [18–20]. Communication protocol IEC 61850 allows a control & protection application which gives immense results compared to conventional solutions. High-speed communications between IEDs connected between substations based on LAN on the exchange of messages (GOOSE) successfully used to replace conventional hardware's for various control & protection applications. SMV communicated from MUs to various protection equipment's at the substation replaces the copper wiring between the CTs/PTs in the yard of substation and the IEDs [21–24]. Two-level control architecture have been proposed in [25] using MATLAB/SIMULINK, where the primary controller is installed at distribution transformer that generates suitable control strategies to deal with distribution network challenges such as load shedding/load reconnection based on available power at the substation, load balancing, protection of feeder against overcurrent and detection of power theft and secondary controller is installed at distribution substation that continuously checks available power and instructs primary controllers for load shedding/load reconnection based on the total connected load on the feeder.

In this work, the architecture of the proposed smart distribution system has been proposed. In this system, Phasor Measurement Unit (PMU) has been placed at the main substation receiving supply from the grid through the incoming feeder, as well as at all distribution transformers (DTs). PMU installed at the main substation is linked to master controller (secondary controller) through IEC 61850 communication protocol. PMUs placed at DTs are connected to the corresponding local controller (primary controller) through the IEC 61850 communication protocol. PMUs are also linked with the smart meters using PLC communication link. PLC communications were typically proprietary, with each supplier having their own closed connections and

protocol (Ethernet TCP/IP). Estimated voltage and current phasors together with frequency are transmitted from PMU to the similar controller through an IEC 61850 communication protocol. Controllers perform different tasks based on the data received from PMUs. Each local controller is linked to master controller as well as to all smart meters placed at loads supplied by the DT. Bidirectional exchange of information takes place between master and local controllers as well as between local controller and smart meter. In this paper, available power at the substation and distribution transformer is developed in real-time with the help of PMU through eMEGASim® OP5600 OPAL-RT real-time simulator. This developed available power in real-time helps in further state estimation such as phase identification and balancing, protection of feeder against overcurrent, detection of power theft and meter tampering, fault detection and isolation, load shedding/load reconnection, billing based on power consumption in the distribution network.

2. THE PROPOSED DISTRIBUTION SYSTEM

In the proposed distribution system (shown in Figure 1), primary controllers (local controllers) are placed at all the distribution transformers (DTs), whereas, the secondary controller (master controller) is situated at the main substation receiving supply from the grid through the incoming feeder. The master controller is linked to n number of local controllers placed at respective DTs.

Local controller 1 placed at first distribution transformer (DT_1) is linked to p number of loads fed by DT_1. Local controller 2 placed at second distribution transformer (DT_2) is linked to q number of loads supplied by DT_2. Local controller placed at nth distribution transformer

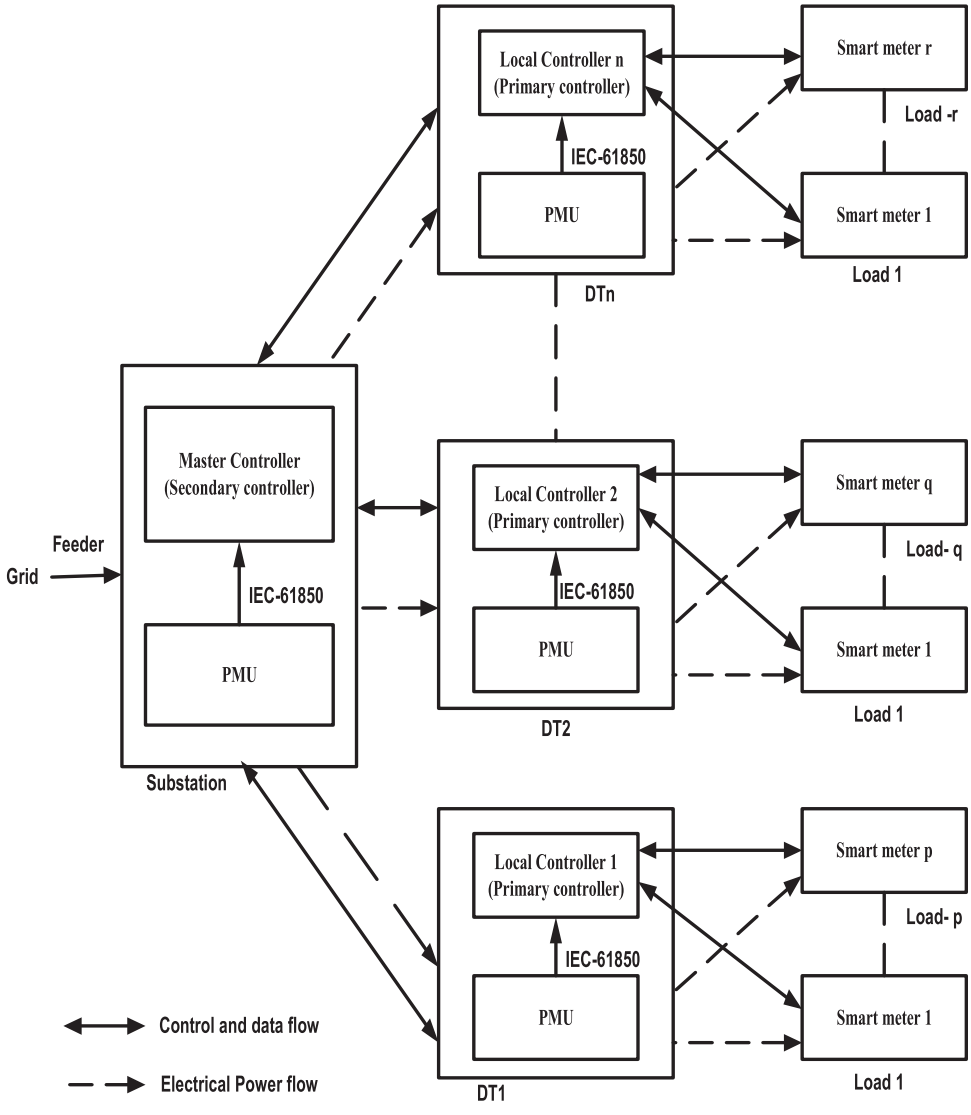

Figure 1: The layout of the proposed distribution system

(DT_n) is linked to r number of loads fed by DT_n. Each load is connected to a smart meter for measurement of various electrical quantities such as voltage, current, real and reactive power consumption, and power factor. Smart meters can interact with local controllers through an IEC-61850 communication protocol. Smart meters are linked to the primary controller (local controller) installed at DT through the communication channel which provides the path for the bidirectional flow of information (data and control signals) between the smart meter and local controller. All local controllers installed at DTs are linked to master controller installed at substation via communication links which provide the path for the bidirectional flow of information between the master controller and local controllers. Master controller compares available power received from the feeder with the total connected load on the substation (data collected from local controllers through smart meters) and instructs local controllers installed at DTs to disconnect/reconnect loads based on available power at the substation. Total available power at the substation is distributed proportionately to all DTs based on the total connected load on each distribution transformer.

Available power in a phase ($P_{available}$) at the substation is given by [25]:

$$P_{\text{available}} = V_{\text{ph}} I_{\text{ph}} \cos \text{Ø} \quad (1)$$

where V_{ph} = Magnitude of phase voltage available at the substation transformer secondary winding (winding on load side); I_{ph} = Magnitude of the phase current of the substation transformer secondary winding; cosØ = Power factor of the phase at the substation transformer secondary winding.

It is apparent from (1) that the reduction of supply voltage/power factor at the substation causes loss of available power, thus requiring load shedding to be performed. To avoid this, loads have been disconnected once available power in a phase differs from the total connected load on that phase by 10% or more. Loads have been reconnected once this difference becomes less than 10%.

Based on information received from the master controller regarding available power, local controllers perform the task of load shedding/load reconnection with due consideration of priority of loads, as per the following algorithm [25]:

(1) If available power in phase A is less than the total connected load on phase A by 10%, go to step 2, else go to step 5.
(2) Find and shut down the load on phase A, which is approximately equal to the difference between total load (in kW) connected on phase A and available power in phase A (in kW). If found, go to step 3, else go to step 4.
(3) Check the priority of that load. If the priority of the load is least, disconnect it immediately, and go to step 1. If the load has a medium priority, wait for a few seconds, if available power becomes normal, go to step 1, else disconnect it and go to step 1. If the load has top priority, don't disconnect it and go to the next step.
(4) Search for the next higher load on phase A, and go to step 3.
(5) Repeat all steps 1–4 for phase B and phase C, respectively.

IEC 61850 is the normal communication protocol *i.e.* employed in substations for communications. It permits combination of control & protection beside its perceptive functions in the substation, and conjointly delivers the resources for super-speed substation security uses, interlocking and inter-tripping. It conjointly permits the relays integration within the IEC 61850-based SAS with numerous vendors MU above IEC 61850 Process Bus. It merges quality of LAN with its capability and protection that's crucial for substations these days. In IEC 61850, relays are inherent into the LAN/Ethernet card with the necessity of LAN equipments like grade switches. In IEC 61850, GOOSE messages are employed for inter-locking, disturbance recording cross-triggering, directional comparison bus protection, failure of breaker protection tripping beside numerous new progressive applications, this helps in removing widespread hardwiring in equipment inlets and helps in reducing the price of distributed protection and management schemes. The execution of IEC GOOSE electronic messaging provides high speed end-to-end transfer. The MUs set on substation yard interface with CTs/PTs sends the voltage/current sampled values over fiber, therefore, eliminating copper wires between primary substation equipments and management, protection, and measure devices.

The devices of SAS are often organized in 3 levels, *e.g.* the station, bay and process level as shown in Figure 2. Within the station level, a user-interface system with database/information, server, workstation, and engineering facilities is put in. The control & protection IEDs, PMUs are put in at the bay level. Process level devices embrace the sensors, CT, VT, CB and MUs. IEC 61850 based protocols are mostly employed by substation automation facilities, *e.g.* GOOSE, SMV and MMS. GOOSE is employed to send tripping signals from

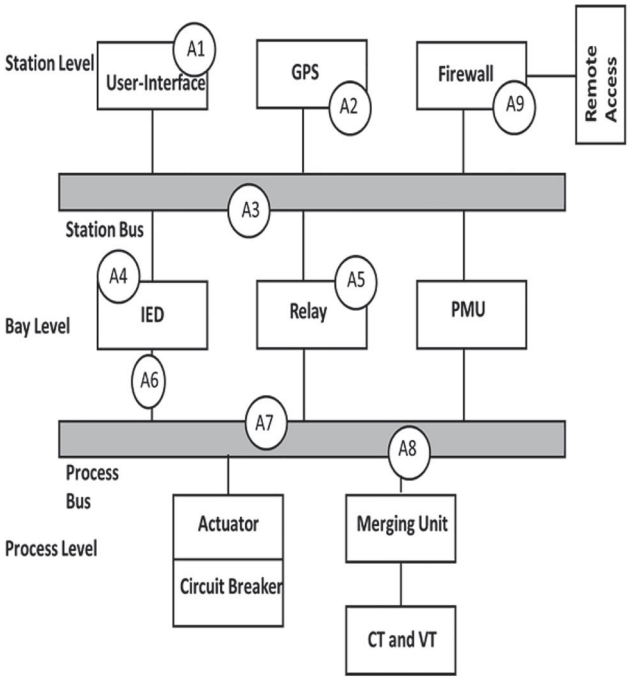

Figure 2: Substation automation system through IEC 61850 communication protocol

IEDs to circuit breakers. Sampled measured voltages and current values are sent from MU to an IED. Several devices are synchronic by GPS.

The substation automation network as illustrated in Figure 2 includes:

A1: Compromise user-interface
A2: Interrupt time synchronization
A3: Compromise station level communication bus
A4: Gain access to bay level devices
A5: change protective device settings
A6: Capture and modify GOOSE message
A7: Compromise process level communication bus
A8: Generate fabricated analog values (SV)
A9: Compromise firewall & gain access to substation

3. CASE STUDIES

Case studies were performed on a distribution test system shown in Figure 3. Considered test system consists of two identical areas each comprising of 21 loads fed through the three-phase radial distributor of 3.5 km (2.175 miles) length having the series impedance (Z) of (0.1535 + j0.3849) ohms/mile [25,26]. Each area contains a combination of top priority, medium priority and least priority loads.

Load details of an area for phase A, phase B, and phase C have been shown in Tables 1–3, respectively [25]. Total sanctioned (maximum load sanctioned by supplier) real

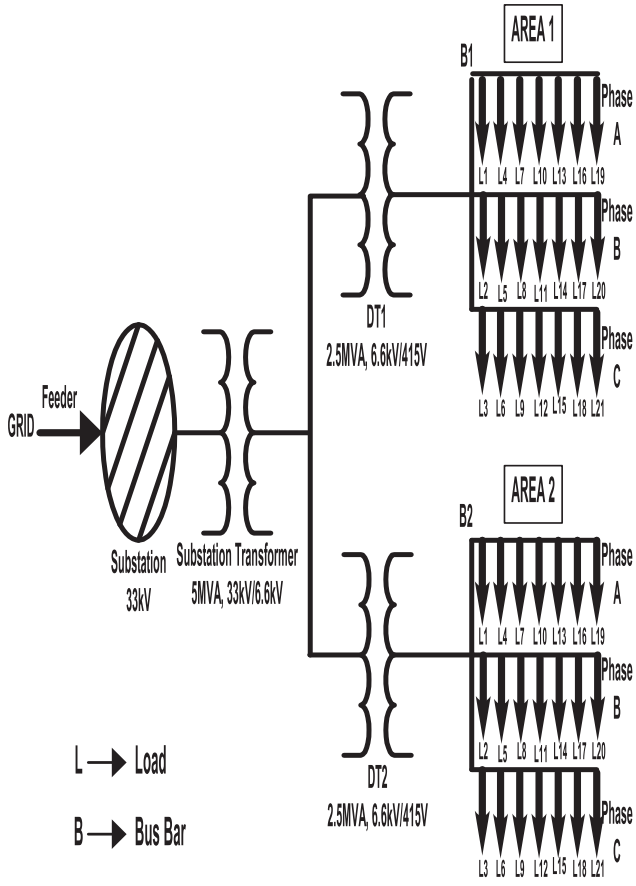

Figure 3: Single line diagram of the proposed distribution test system [25]

Table 1: Load details of area 1/area 2 for phase A [25]

Load on phase A

Load number	Connected load kW	Connected load kVAR	Sanctioned load kW	Sanctioned load kVAR	Load priority[a]
1	105	45	110	50	2
4	90	25	105	30	2
7	95	55	100	60	1
10	120	55	130	60	3
13	110	50	110	55	3
16	100	35	100	40	3
19	95	50	100	55	3
Total	715	315	755	350	

[a] 1 – Top priority, 2 – Medium priority, 3 – Least priority

and reactive power demands in an area are 2265 kW and 1050kVAR, respectively, with the real and reactive power demand of 755 kW and 350 kVAR, respectively, on each phase. Total connected (actual connected load of the consumer which is less than maximum sanctioned demand) real power demand and reactive power demand in an area are 2145 kW and 945 kVAR, respectively, with the real and reactive power demand of 715 kW and 315 kVAR, respectively, on each phase. Each load is placed with a smart meter. Two areas are fed through distribution transformers DT_1 and DT_2, respectively, each

Table 2: Load details of area 1/area 2 for phase B [25]

Load on phase B					
	Connected load		Sanctioned load		
Load number	kW	kVAR	kW	kVAR	Load priority[a]
2	125	60	135	65	1
5	100	50	105	55	2
8	120	65	125	70	3
11	85	35	95	40	2
14	90	35	90	40	3
17	80	35	90	40	3
20	115	35	115	40	3
Total	715	315	755	350	

[a]1 – Top priority, 2 – Medium priority, 3 – Least priority

Table 3: Load details of area 1/area 2 for phase C [25]

Load on phase C					
	Connected load		Sanctioned load		
Load number	kW	kVAR	kW	kVAR	Load priority[a]
3	75	35	75	40	2
6	130	55	140	60	2
9	90	45	95	50	3
12	120	45	135	50	2
15	105	45	105	50	3
18	100	45	105	50	2
21	95	45	100	50	2
Total	715	315	755	350	

[a]1 – Top priority, 2 – Medium priority, 3 – Least priority

rated 2.5MVA, 50 Hz, 6.6 kV/415 V. Distribution transformers are supplied from 33 kV distribution substation through substation transformer rated 5 MVA, 50 Hz, 33 kV/6.6 kV. The 33 kV distribution substation gets power injected to it from the grid through the 33 kV incoming feeder.

Algorithm presented in section 2 regarding load shedding/load reconnection based on available power were tested on a developed MATLAB/SIMULINK model of the test system as shown in Figure 3 [25] as well as on an eMEGASim® OP5600 OPAL-RT real-time simulator as shown in Figure 4. Simulation results are presented below.

IEC-61850 communication protocol is implemented using OPAL RT which is used as a communication interface to send data to a remote device and receive data from it. This communication protocol is used for communicating between a power system network (substation and distribution transformer) and control center (controller). In this paper, IEC 61850 communication protocol is used in Area 2 to send the data (voltage and current) at the substation and distribution transformer by using Op61850 Merging Unit Mask and SV Subscriber Mask blocks directly to the controller.

(a) The block 'Op61850 Merging Unit Mask' is used to simulate an IEC 61850 Logical Device Merging Unit in a Substation Automation System. According to IEC 61850-9-2-LE document, a merging unit is an interface unit that accepts 4 CT/VT in input and produces time synchronized sampled values on the IEC 61850 network.

(b) The block 'Op61850 Sampled Values Subscriber Mask' is used to subscribe to IEC 61850 Sampled Value messages sent by Logical Device Merging Unit in a Substation Automation System. Block's outputs provide 4 CT/VT time synchronized sampled values as well as the Quality information.

The IEC 61850 communication networks and systems potency automation permits utilities to think about new styles for substations applicable for each new substation and refurbishments. IEC 61850 encompasses two buses supported the LAN technology *i.e.* Station Bus and Process Bus shown in Figure 4. Figure 4 shows the abstract design of a whole IEC 61850 SAS. A high voltage substation supported IEC 61850 process bus shows particular network topology because it pretends to indicate the logical view of IEC 61850 specification. The figure illustrates physically separate networks for Station Bus and Process Bus IED's connected to each network via freelance network interfaces. But it's potential that Station Bus and Process Bus are within the same physical network sharing a typical set of LAN switches. The IEC 61850 Station Bus interconnects all bays with the station higher-up level and carries management in sequence like measurement, interlocking and operations. Station Bus introduces many advantages just like the use of GOOSE messages for quick transfer of essential protection information. GOOSE has been employed in this paper for exchanging between IEDs interlocking and obstruction signals, as it permits reduction of copper wiring conventionally used for exchanging binary information among relays due to the use of Ethernet network. The IEC 61850 Process Bus interconnects the IEDs among a bay that carries real-time measurements for security known as Sampled Values (SV). Process Bus goes a step further than Station Bus because it provides the digital link to the apparatus like switchgear and instrument transformers. It not solely reduces copper wiring among the switchyard however conjointly makes safer and easier the upkeep of IED panel on top of things by eliminating high energy signals. Relay panels have abundant less wiring that helps in regulate the sign of the interfaces between primary and secondary systems.

3.1 Phasor Measurement Unit (PMU)

The PMU calculates the phase, magnitude, frequency and ROCOF of the positive sequence component of

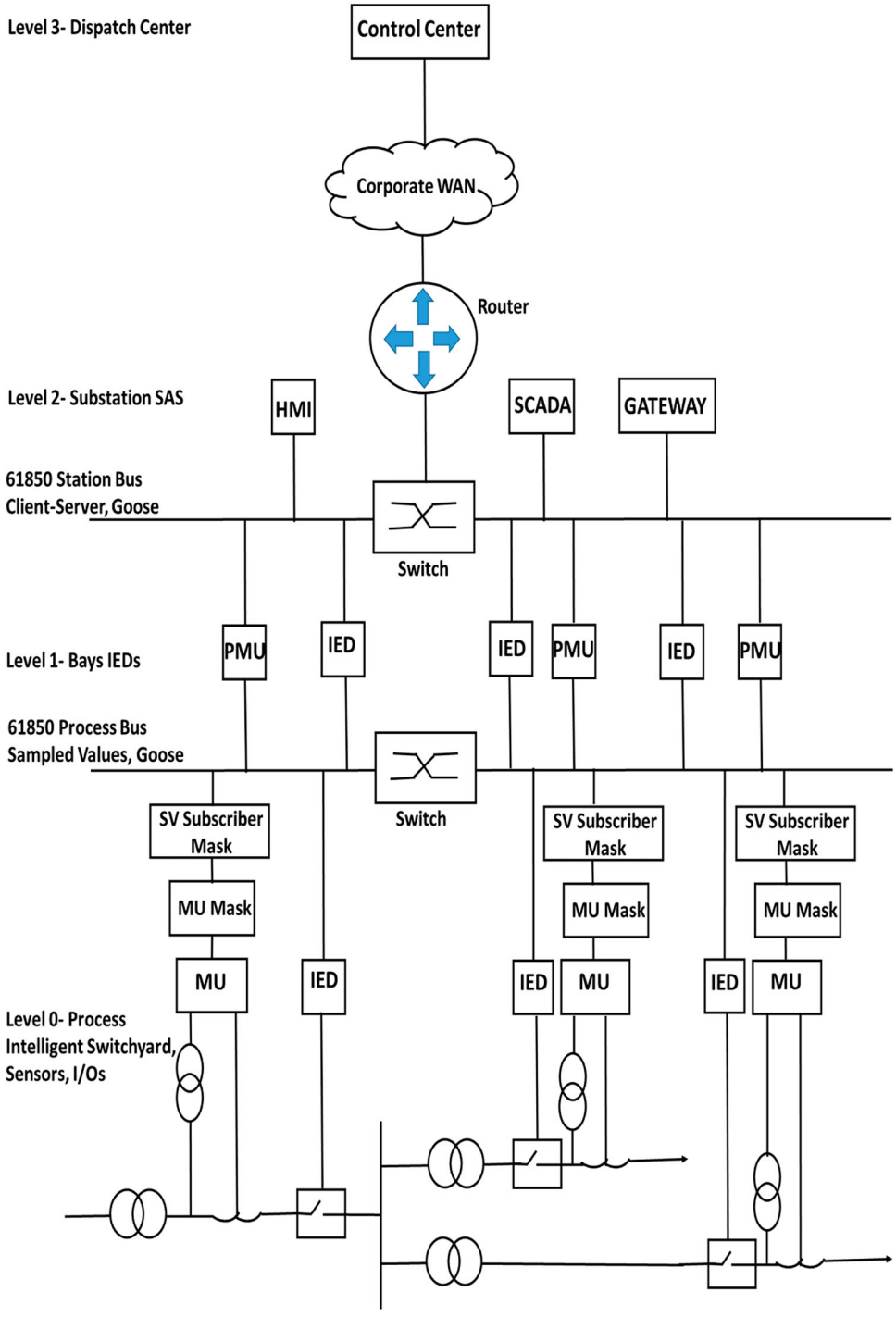

Figure 4: Layout of the proposed distribution system with IEC 61850 communication protocol

three-phase voltage/current signal. PMU block uses PLL to determine the component of frequency and a positive-sequence measurement over a running window of one cycle of the fundamental frequency. Input to the PMU is the three-phase signal (pu) with 50 Hz nominal frequency. The three outputs of the PMU block is the magnitude of the positive-sequence signal (pu), phase (degrees relative to the PLL phase) and frequency (Hz). Here, in this paper, the PMU is placed at the substation and distribution transformer to determine the available power at the substation and at distribution transformer.

3.1.1 *Available Power at the Substation with the Help of PMU*

Simulation results for calculation of available power through PMU in real-time at the substation by considering the load disconnection/connection based on available power (from time $t = 0.56$sec to time $t = 0.75$sec),

protection of feeder against overcurrent (from time $t = 0.15$sec to time $t = 0.20$sec), and Power theft detection and elimination (from time $t = 0.21$sec to time $t = 0.23$sec) have been shown below.

3.1.1.1 Input Voltage and Current to PMU at Substation. The input three-phase voltage signal $V_{\text{rms}} = 3600$ V with 50 Hz nominal frequency at the substation is shown in Figure 5.

The input three-phase current signal $I_{\text{rms}} = 300$A with 50 Hz nominal frequency at the substation is shown in Figure 6. It is observed from Figure 6, that there is an overcurrent from time $t = 0.15$sec to time $t = 0.20$sec due to the connection of an extra load consisting of real power demand and reactive power demand of 150 kW and 150kVAR, respectively, to load number 1 of phase A in area 1. Also, there is power theft in Phase C, due to the connection of illegal load of real and reactive power load of 150 kW and 80kVAR respectively at time $t = 0.21$sec and was removed at time $t = 0.23$sec. It is also observed from Figure 6 that the load disconnected based on available power from time $t = 0.56$sec and is reconnected at time $t = 0.75$sec.

3.1.1.2 PMU Output – Magnitude of the Voltage and Current at Substation. The magnitude of the positive-sequence voltage signal at the substation is shown in Figure 7.

The magnitude of the positive-sequence current signal at the substation is shown in Figure 8. And, it is observed from the magnitude of current in Figure 8, that there is an overcurrent from time $t = 0.15$sec to time $t = 0.20$sec due to the connection of an extra load consisting of real power demand and reactive power demand of 150 kW

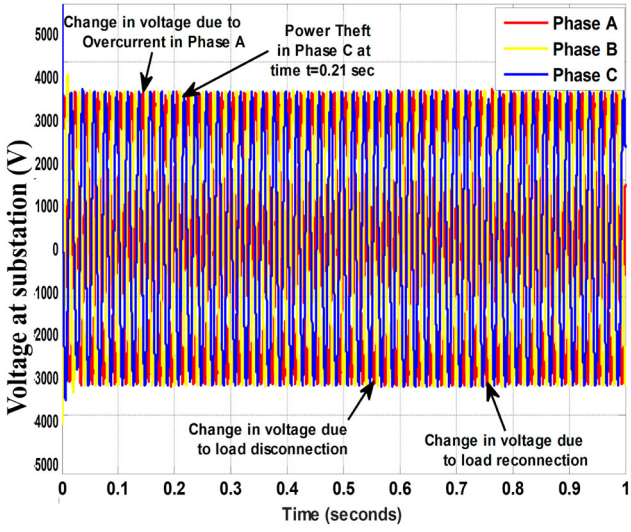

Figure 5: Input voltage to PMU at the substation

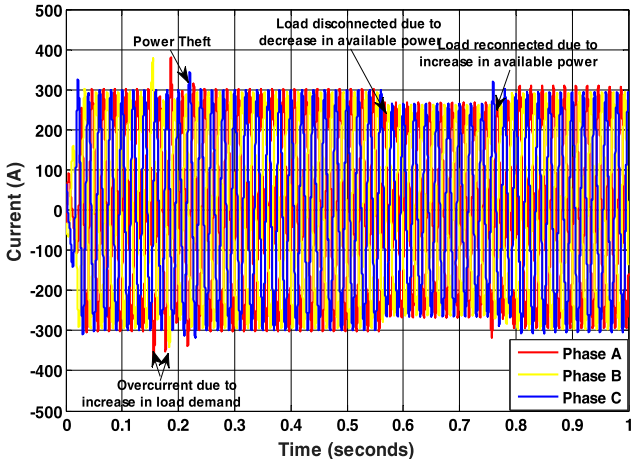

Figure 6: Input current to PMU at the substation

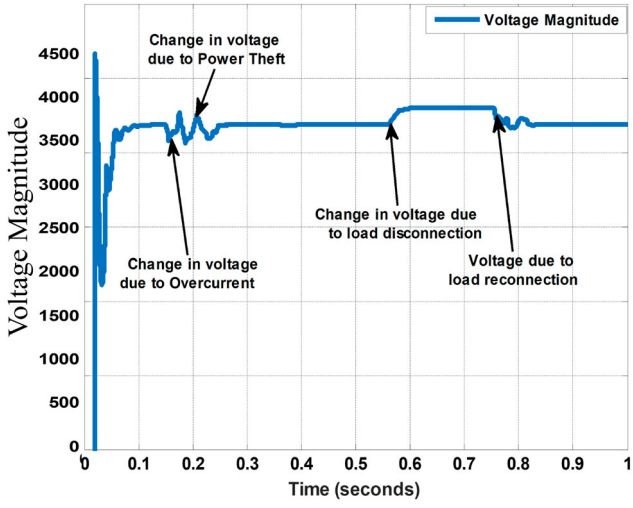

Figure 7: Magnitude of the voltage at the substation

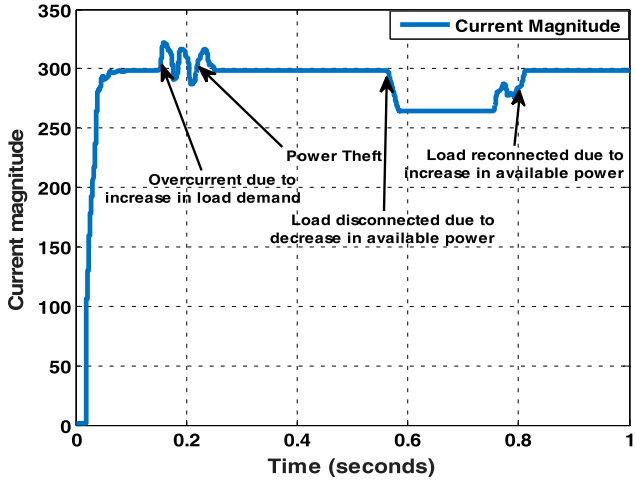

Figure 8: Magnitude of current at the substation

and 150kVAR, respectively, to load number 1 of phase A in area 1. Also, there is power theft in Phase C, due to the connection of illegal load of real and reactive power load of 150 kW and 80kVAR respectively at time $t = 0.21$sec and was removed at time $t = 0.23$sec. It is also observed from Figure 8 that the load disconnected based on available power from time $t = 0.56$sec and is reconnected at time $t = 0.75$sec.

3.1.1.3 PMU Output – Phase Angle of Voltage and Current at Substation. The phase angle (degrees relative to the PLL phase) of the three-phase voltage signal at the substation is shown in Figure 9. And, it is observed from Figure 9 that the phase angle w.r.t. time reaches to −0.78 degree due to transients at the instant of starting and then it becomes normal with some variations due to variations in load.

The phase angle (degrees relative to the PLL phase) of the three-phase current signal at the substation is shown in Figure 10. And, it is observed from Figure 10 that the phase angle w.r.t. time reaches to −59.89 degree due to transients at the instant of starting and then it becomes normal with some variations due to variations in load.

3.1.1.4 PMU Output – Frequency (Hz) of Voltage and Current at Substation. According to the Standards for Power Frequency in India, the nominal frequency of operation in Indian grid is 50.0 Hz and the permissible frequency band specified by Indian Electricity Grid Code (IEGC) is 49.5 to 50.2 Hz. The frequency (Hz) of the three-phase voltage signal at the substation is shown in Figure 11. And, it is observed from Figure 11, that frequency of voltage signal at substation varies from 49.9

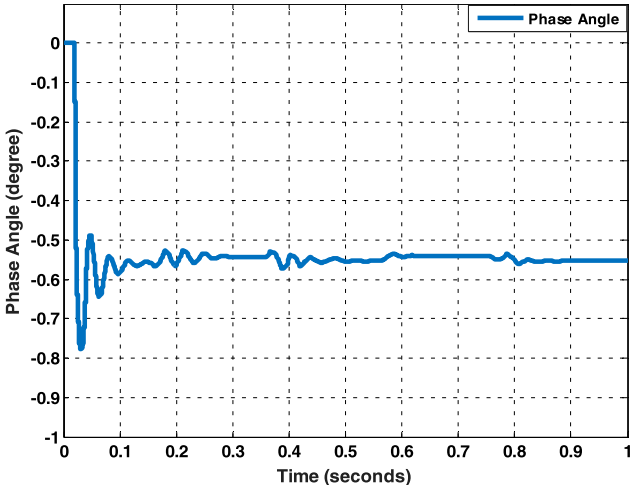

Figure 9: The phase angle of the voltage at the substation

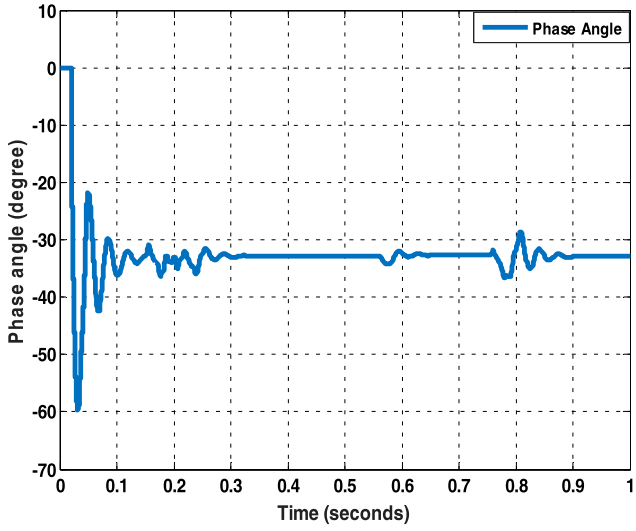

Figure 10: The phase angle of current at the substation

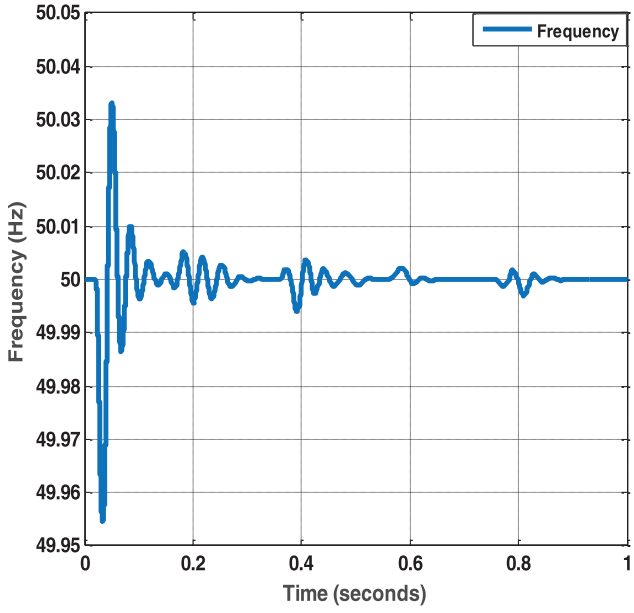

Figure 11: The rate of change of frequency of the voltage at the substation

to 50.03 Hz *i.e.* within the permissible frequency band specified by IEGC.

The frequency (Hz) of the three-phase current signal at the substation is shown in Figure 12. And, it is observed from Figure 12, that the frequency of current signal is within the permissible frequency band specified by IEGC but there is a slight variation in frequency due to overcurrent from time $t = 0.15$sec to time $t = 0.20$sec. It is seen from the Figure 12, that load is disconnected from time $t = 0.56$sec and is reconnected from time $t = 0.75$sec. After reconnection of load, there is a slight increase in the frequency which crosses the permissible frequency band

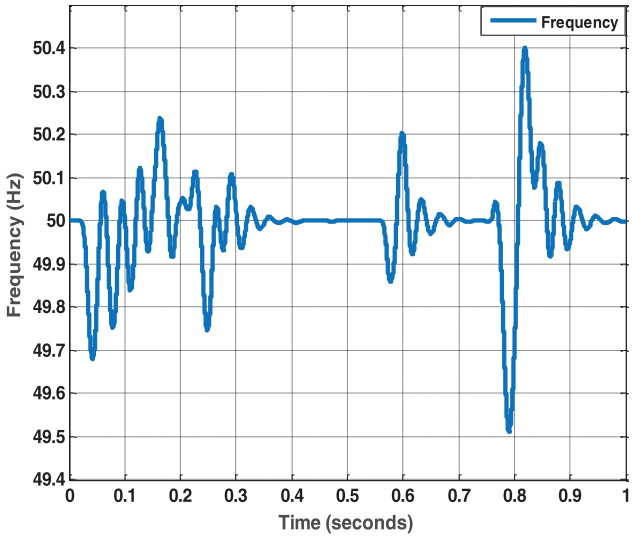

Figure 12: The rate of change of frequency of the current at the substation

specified by IEGC, so there is need of frequency control. So, at time $t = 0.82$sec by using load frequency control method, the frequency comes within the permissible frequency band specified by IEGC.

3.1.1.5 Power Factor and Available Power at the Substation. The power factor at the substation is shown in Figure 13. It is observed from Figure 13, that power factor reaches to 0.51 due to transients at the instant of starting and after that power factor at the substation maintains between ranges 0.8–0.9.

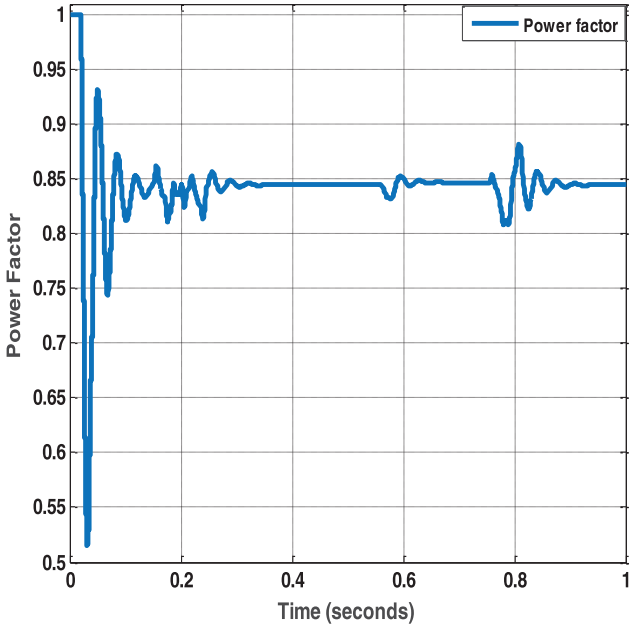

Figure 13: Power factor at the substation

The available power at the substation is shown in Figure 14. Available power in a phase ($P_{\text{available}}$) at the substation is given by equation (1) *i.e.* $P_{\text{available}} = V_{\text{ph}} I_{\text{ph}}$ cosØ. It is observed from Figure 14, that the reduction of supply voltage/power factor at the substation causes loss of available power, thus requiring load shedding to be performed.

The master controller continuously checked total available power at the substation and decided the distribution of available power to distribution transformers DT_1 and DT_2 connected to two areas based on the total connected load in each area. It is observed from Figure 14 that available power drops from 3.2MW to 2.8MW at time $t = 0.56$sec. Since available power is less than total connected load by 11.3%, master controller present at substation instructs local controller at DT_1 to perform load shedding as per algorithm presented in section 2. It is observed from Figure 14 that available power is recovered to 3.2MW at time $t = 0.75$sec. So, load is disconnected based on available power from time $t = 0.56$sec and is reconnected at time $t = 0.75$sec.

It is observed from Figure 14, that there is an overcurrent from time $t = 0.15$sec to time $t = 0.20$sec due to the connection of an extra load consisting of real power demand and reactive power demand of 150 kW and 150kVAR, respectively, to load number 1 of phase A in area 1. Also, there is power theft in Phase C, due to the connection of illegal load of real and reactive power load of 150 kW and 80kVAR respectively at time $t = 0.21$sec and was removed at time $t = 0.23$sec.

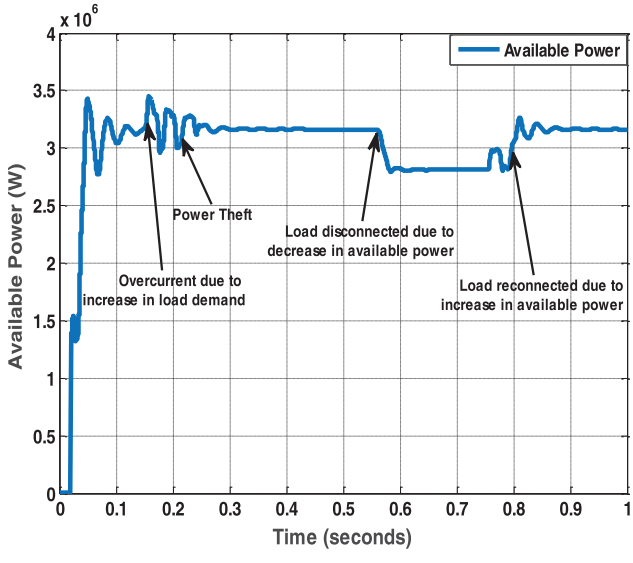

Figure 14: Available power at the substation

It has been shown from Figure 14 that, the available power simulated from MATLAB /SIMULINK closely matches with the available power calculated by real-time PMU at the substation.

3.1.2 Available Power at the Distribution Transformer with the Help of PMU

Simulation results for calculation of available power through PMU in real-time at the distribution transformer by considering the load disconnection/connection based on available power (from time $t = 0.56$sec to time $t = 0.75$sec), protection of feeder against overcurrent (from time $t = 0.15$sec to time $t = 0.20$sec), and Power theft detection and elimination (from time $t = 0.21$sec to time $t = 0.23$sec) have been shown below.

3.1.2.1 Input Voltage and Current to PMU at DT_1. The input three-phase voltage signal $V_{\text{rms}} = 243.4$ V with 50 Hz nominal frequency at DT_1 is shown in Figure 15.

The input three-phase current signal $I_{\text{rms}} = 3500$A with 50 Hz nominal frequency at the DT_1 is shown in Figure 16. It is observed from Figure 16, that there is an overcurrent from time $t = 0.15$sec to time $t = 0.20$sec due to the connection of an extra load consisting of real power demand and reactive power demand of 150 kW and 150kVAR, respectively, to load number 1 of phase A in area 1. Also, there is power theft in Phase C, due to the connection of illegal load of real and reactive power load of 150 kW and 80kVAR respectively at time $t = 0.21$sec and was removed at time $t = 0.23$sec. It is also observed from Figure 16 that the load disconnected based on available power from time $t = 0.56$sec and is reconnected at time $t = 0.75$sec.

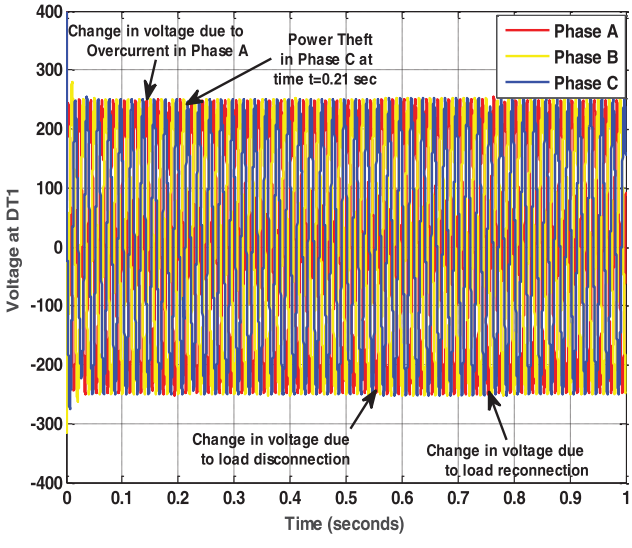

Figure 15: Input voltage to PMU at DT_1

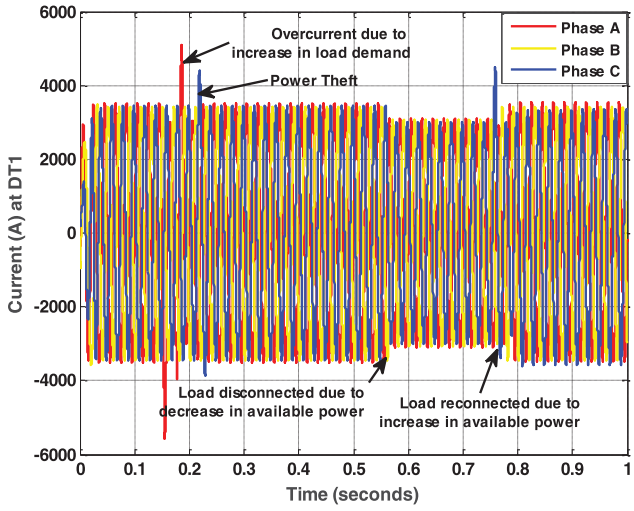

Figure 16: Input current to PMU at DT_1

3.1.2.2 PMU Output – Magnitude of Voltage and Current at DT_1. The magnitude of the positive-sequence voltage signal at DT_1 is shown in Figure 17.

The magnitude of the positive-sequence current signal at the DT_1 is shown in Figure 18. And, it is observed from the magnitude of current in Figure 18, that there is an overcurrent from time $t = 0.15$sec to time $t = 0.20$sec due to the connection of an extra load consisting of real power demand and reactive power demand of 150 kW and 150kVAR, respectively, to load number 1 of phase A in area 1. Also, there is power theft in Phase C, due to the connection of illegal load of real and reactive power load of 150 kW and 80kVAR respectively at time $t = 0.21$sec and was removed at time $t = 0.23$sec. It is also observed from Figure 18 that the load disconnected

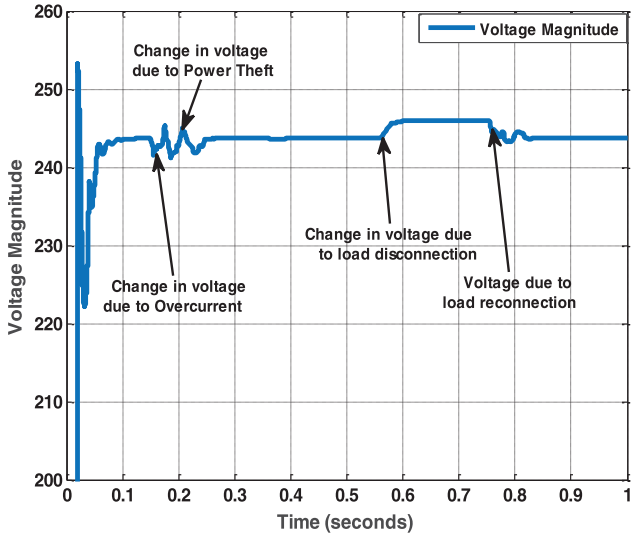

Figure 17: Magnitude of the voltage at DT_1

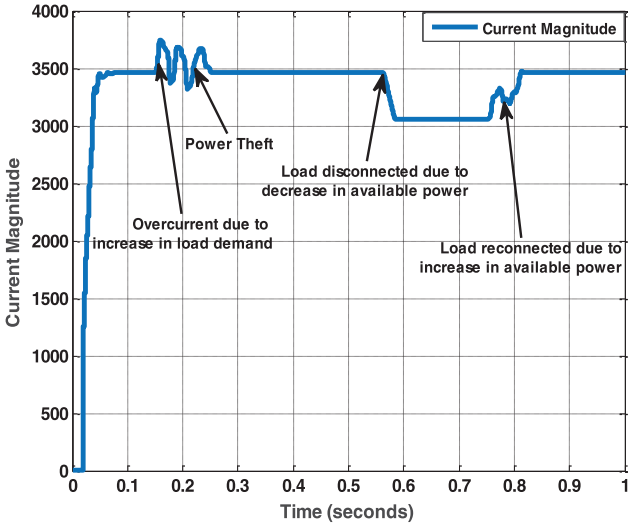

Figure 18: The magnitude of the current at DT_1

based on available power from time $t = 0.56$sec and is reconnected at time $t = 0.75$sec.

3.1.2.3 PMU Output – Phase Angle of Voltage and Current at DT_1. The phase (degrees relative to the PLL phase) of the three-phase voltage signal at the DT_1 is shown in Figure 19. And, it is observed from Figure 19 that the phase angle w.r.t. time reaches to 46 degree due to transients at the instant of starting and then it becomes normal with some variations due to variations in load.

The phase (degrees relative to the PLL phase) of the three phase current signal at the DT_1 is shown in Figure 20. And, it is observed from Figure 20 that the phase angle w.r.t. time varies from −18 to 7 degree due to transients at the instant of starting and then it becomes normal with some variations due to variations in load.

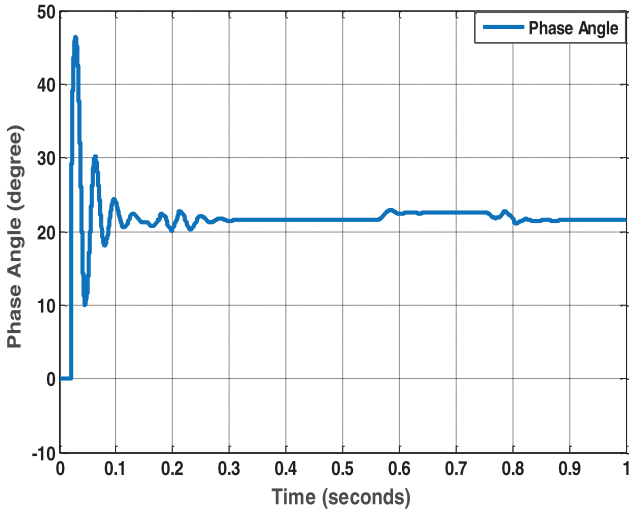

Figure 19: The phase angle of the voltage at DT_1

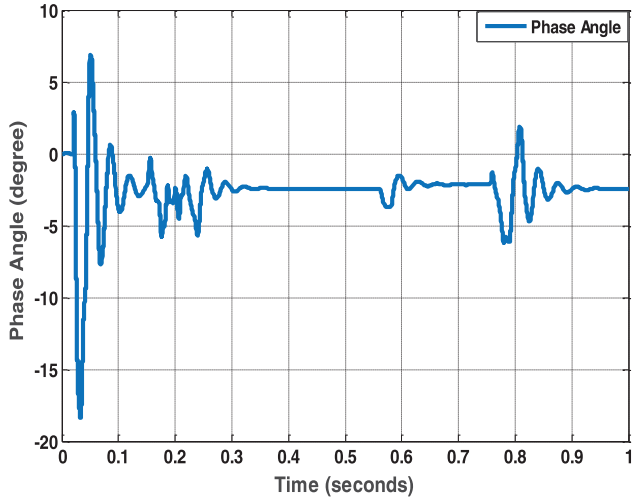

Figure 20: The phase angle of current at DT_1

3.1.2.4 PMU Output – Frequency of Voltage and Current at DT_1. The frequency (Hz) of the three-phase voltage signal at the DT_1 is shown in Figure 21. According to the Standards for Power Frequency in India, the nominal frequency of operation in Indian grid is 50.0 Hz and the permissible frequency band specified by Indian Electricity Grid Code (IEGC) is 49.5 to 50.2 Hz. The frequency (Hz) of the three-phase voltage signal at the DT_1 is shown in Figure 21. And, it is observed from Figure 21, that frequency of voltage signal at DT_1 varies from 49.8 to 50.2 Hz *i.e.* within the permissible frequency band specified by IEGC.

The frequency (Hz) of the three-phase current signal at the DT_1 is shown in Figure 22. And, it is observed from Figure 22, that the frequency of current signal is within

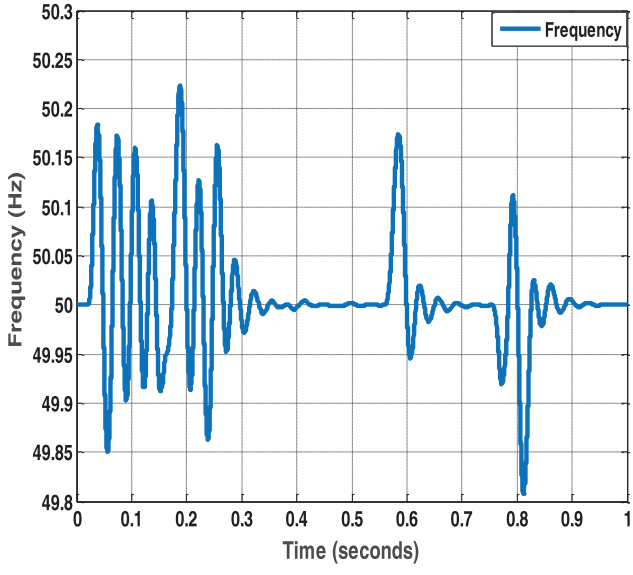

Figure 21: The rate of change of frequency at DT_1

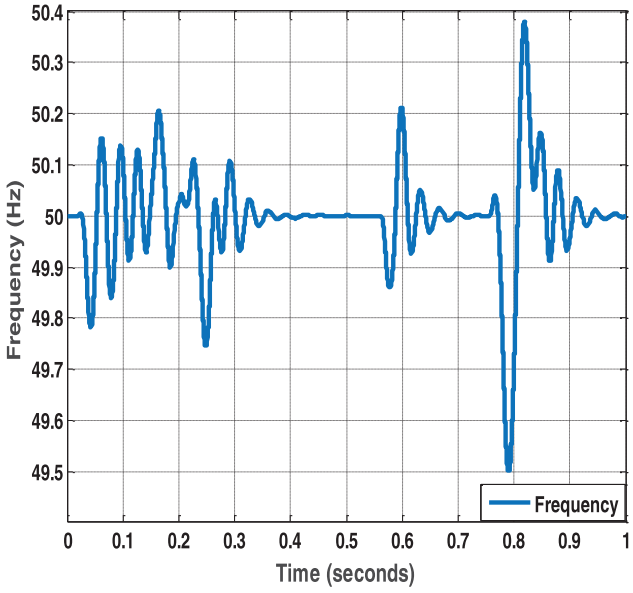

Figure 22: The rate of change of frequency at DT_1

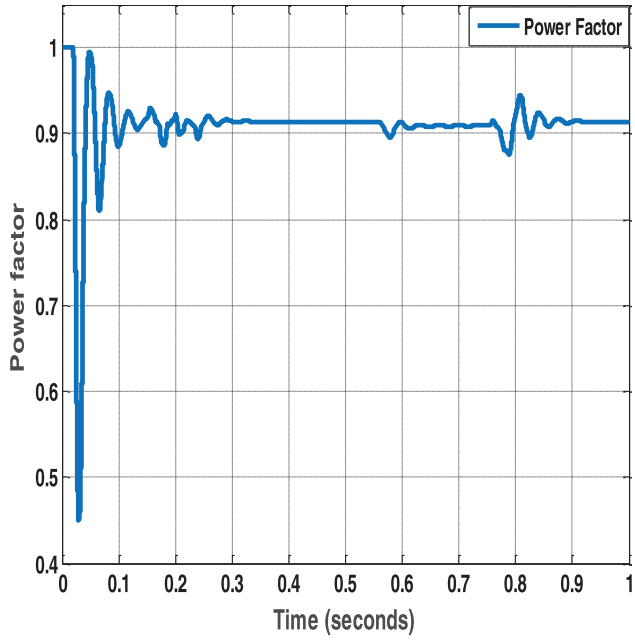

Figure 23: Power factor at DT_1

the permissible frequency band specified by IEGC but there is a slight variation in frequency due to the disconnection of load from time $t = 0.56$sec and its reconnection from time $t = 0.75$sec. After reconnection of load there is a slight increase in the frequency which crosses the permissible frequency band specified by IEGC, so there is need of frequency control. So, at time $t = 0.82$sec by using load frequency control method, the frequency comes within the permissible frequency band specified by IEGC.

3.1.2.5 Power Factor and Available Power at the DT_1.

The power factor at DT_1 is shown in Figure 23. It is observed from Figure 23, that power factor reaches to 0.46 due to transients at the instant of starting and after that power factor at the DT_1 maintains between ranges 0.89–0.95.

The available power at the substation is shown in Figure 24. Available power in a phase ($P_{available}$) at the DT_1 is given by Equation (1) *i.e.* $P_{available} = V_{ph}\ I_{ph}$ cosØ. It is observed from Figure 24, that the reduction of supply voltage/power factor at the substation causes loss of available power, thus requiring load shedding to be performed.

The master controller continuously checked total available power at the substation and decided the distribution of available power to distribution transformers DT_1 and DT_2 connected to two areas based on the total connected load in each area. It is observed from Figure 24 that available power drops from 2.4MW to 2.09MW at

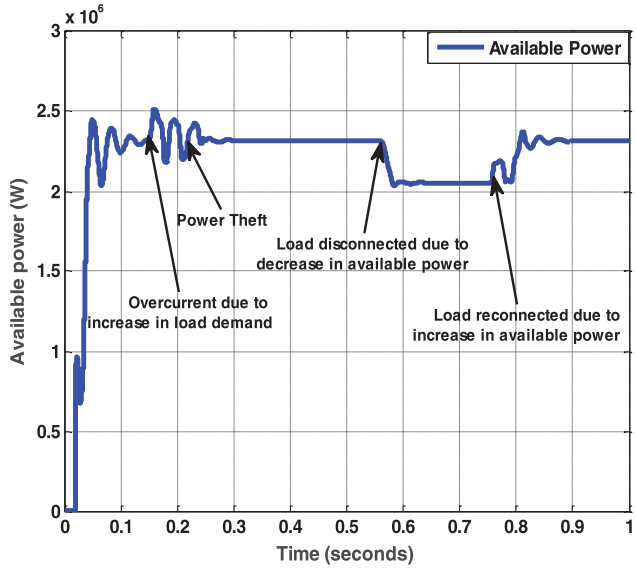

Figure 24: Available power at DT_1

time $t = 0.56$sec. Since available power is less than total connected load by 11.3%, master controller present at substation instructs local controller at DT_1 to perform load shedding as per algorithm presented in Section 2. It is observed from Figure 24 that available power is recovered to 2.4MW at time $t = 0.75$sec. So, load is disconnected based on available power from time $t = 0.56$sec and is reconnected at time $t = 0.75$sec.

It is observed from Figure 24, that there is an overcurrent from time $t = 0.15$sec to time $t = 0.20$sec due

to the connection of an extra load consisting of real power demand and reactive power demand of 150 kW and 150kVAR, respectively, to load number 1 of phase A in area 1. Also, there is power theft in Phase C, due to the connection of illegal load of real and reactive power load of 150 kW and 80kVAR respectively at time $t = 0.21$sec and was removed at time $t = 0.23$sec.

It has been shown from Figure 24 that, the available power simulated from MATLAB/SIMULINK closely matches with the available power calculated by real-time PMU at the distribution transformer.

4. CONCLUSIONS

An architecture of the distribution system has been proposed, where PMU has been placed at the main substation receiving supply from the grid through the incoming feeder, as well as at all DTs. PMU installed at the main substation is linked to master controller (secondary controller) through IEC 61850 communication protocol. PMUs placed at DTs are connected to the corresponding local controller (primary controller) through the IEC 61850 communication protocol. Estimated voltage and current phasors together with frequency are transmitted from PMU to the local controller through IEC 61850 communication protocol. Controllers perform different tasks based on the data received from PMUs. In this paper, information about the available power at the substation and distribution transformer is developed in real-time with the help of PMU by considering the load disconnection/connection based on available power (from time $t = 0.56$sec to time $t = 0.75$sec), protection of feeder against overcurrent (from time $t = 0.15$sec to time $t = 0.20$sec), and power theft detection and elimination (from time $t = 0.21$sec to time $t = 0.23$sec) through eMEGASim® OP5600 OPAL-RT real-time simulator.

This developed available power in real-time helps in determining how total available power at the substation is distributed proportionately to all DTs based on the total connected load on each distribution transformer on its three phases. It also helps in phase identification and balancing, protection of feeder against overcurrent, detection of power theft and meter tampering, fault detection and isolation, load shedding/load reconnection, billing based on power consumption in the distribution network.

ORCID

Alok Jain http://orcid.org/0000-0001-9465-6884

REFERENCES

1. G. T. Costanzo, G. Zhu, M. F. Anjos, and G. Savard, "A system architecture for autonomous demand-side load management in smart buildings," *IEEE Trans. Smart Grid*, Vol. 3, no. 4, pp. 2157–65, Dec. 2012.

2. Y. Wang, W. Saad, N. B. Mandayam, and H. Vincent Poor, "Load shifting in the smart grid: To participate or not," *IEEE Trans. Smart Grid*, Vol. 7, no. 6, pp. 2604–14, Nov. 2016.

3. A. Safdarian, M. Fotuhi-Firuzabad, and M. Lehtonen, "A distributed algorithm for managing residential demand response in smart grids," *IEEE Trans. Ind. Inf.*, Vol. 10, no. 4, pp. 2385–93, Nov. 2014.

4. A. Safdarian, M. Fotuhi-Firuzabad, and M. Lehtonen, "Optimal residential load management in smart grids: a decentralized framework," *IEEE Trans. Smart Grid*, Vol. 7, no. 4, pp. 1386–845, July 2016.

5. V. Arya, D. Seetharam, S. Kalyanaraman, K. Dontas, C. Pavlovski, S. Hoy, and J. R. Kalagnanam, "Phase identification in smart grids," *IEEE International Conference on Smart Grid Communications*, Brussels, Belgium, Oct. 2011.

6. H. Pezeshki and P. J. Wolfs, "Consumer phase identification in a three-phase unbalanced LV distribution network," *IEEE PES Innovative Smart Grid Technologies*, Berlin, Germany, Europe, 2012, pp. 1–7.

7. W. Wang, N. Yu, and B. Foggo, "Phase identification in electric power distribution systems by clustering of smart meter data," *IEEE International Conference on Machine Learning and Applications*, Anaheim, CA, USA, 2016, pp. 259–265.

8. T. A. Short, "Advanced metering for phase identification, transformer identification and secondary modeling," *IEEE Trans. Smart Grid*, Vol. 4, no. 2, pp. 651–8, June 2013.

9. J. Ma, H. H. Chen, L. Song, and Y. Li, "Residential load scheduling in smart grid: A cost efficiency perspective," *IEEE Trans. Smart Grid*, Vol. 7, no. 2, pp. 771–84, March 2016.

10. P. K. Lee, and L. L. Lai. "Smart metering in micro-grid applications," *Proceedings of IEEE Power and Energy Society General Meeting*, Calgary, July 2009, pp. 1–5.

11. D. Alahakoon, and X. Yu, "Smart electricity meter data intelligence for future energy systems: A survey," *IEEE Trans. Ind. Inf.*, Vol. 12, no. 1, pp. 425–36, Feb. 2016.

12. M. M. Albu, M. Sănduleac, and C. Stănescu, "Syncretic use of smart meters for power quality monitoring in emerging networks," *IEEE Trans. Smart Grid*, Vol. 8, no. 1, pp. 485–92, Jan. 2017.

13. S. Haben, C. Singleton, and P. Grindrod, "Analysis and clustering of residential customers energy behavioral demand using smart meter data," *IEEE Trans. Smart Grid*, Vol. 7, no. 1, pp. 136–44, Jan. 2016.

14. M. H. J. Bollen, R. Das, S. Djokic, P. Ciufo, J. Meyer, S. K. Rönnberg, and F. Zav, "Power quality concerns in implementing smart distribution-grid applications," *IEEE Trans. Smart Grid*, Vol. 8, no. 1, pp. 391–9, Jan. 2017.

15. X. Liu, M. Shahidehpour, Z. Li, X. Liu, Y. Cao, and W. Tian, "Protection scheme for loop-based microgrids," *IEEE Trans. Smart Grid*, Vol. 8, no. 3, pp. 1340–9, May 2017.

16. P. Jokar, N. Arianpoo, and V. C. M. Leung, "Electricity theft detection in AMI using customers consumption patterns," *IEEE Trans. Smart Grid*, Vol. 7, no. 1, pp. 216–26, Jan. 2016.

17. "IEEE standard for synchrophasor measurements for power systems," IEEE Std C37.118.1-2011, 2011.

18. J. De La Ree, V. Centeno, J. S. Thorp, and A. G. Phadke, "Synchronized phasor measurement applications in power systems," *IEEE Trans. Smart Grid*, Vol. 1, no. 1, pp. 20–7, June 2010.

19. "IEEE standard for synchrophasor data transfer for power systems," IEEE Std C37.118.2-2011, 2011.

20. "IEEE guide for phasor data concentrator requirements for power system protection, control, and monitoring," IEEE Std C37.244-2013, 2013.

21. S. Roostaee, R. Hooshmand, and M. Ataei, "Substation automation system using IEC 61850," *Power Engineering and Optimization Conference*, Shah Alam, Selangor, 6–7 June 2011, pp. 393–7.

22. R. Hughes and M. Jansen, "Engineering processes using IEC 61850," *Australasian Universities Power Engineering Conference*, Adelaide, SA, 2009, pp. 1–6.

23. R. P. Madiba, and L. D. Erasmus, "Organisational impact of implementing IEC 61850 standard for communication networks and systems in substations," in *Proceedings of Technology Management in the IT-Driven Services Conference*, San Jose, CA, USA, Aug. 2013, pp. 2681–9.

24. C. Brunner, "IEC 61850 for power system communication," *IEEE/PES Transmission and Distribution Conference and Exposition*, Chicago, IL, April 2008, pp. 1–6.

25. J. Alok, and M. K. Verma, "Monitoring, control, and protection of radial distribution networks by using a two-level control architecture," *Int. Trans. Electrical Energy Syst.*, Vol. 29, accepted in Sept. 2019.

26. IEEE Distribution System Analysis Subcommittee, "IEEE 13 node test feeder." Available: http://ewh.ieee.org/soc/pes/dsacom/testfeeders.html

Authors

Alok Jain received his BTech (Hons.) degree in electrical & electronics engineering from UPTU, Lucknow, India in 2010 and ME degree in electrical engineering (power systems & electric drives) from Thapar University, Patiala, Punjab, India in 2013. He is currently pursuing a degree in Electrical Engineering Department at Indian Institute of Technology (BHU), Varanasi, India. His research interests include smart grid, smart metering, microgrid, power quality, distributed generation, and renewable energy.

Corresponding author. Email: alok.rs.eee14@itbhu.ac.in

M K Verma received his BSc (Eng.) degree in electrical engineering from Regional Engineering College, Rourkela (presently National Institute of Technology, Rourkela), India in 1989, MSc (Eng.) degree in electrical engineering from Bihar Institute of Technology, Sindri, India in 1994 and PhD degree in electrical engineering from Indian Institute of Technology (IIT), Kanpur, India in 2005. He is currently working as Professor in Electrical Engineering Department at Indian Institute of Technology (BHU), Varanasi, India. His current research interests include voltage stability studies, application of FACTS controllers, power quality, wide area monitoring system and smart grid.

Email: mkverma.eee@iitbhu.ac.in